

# We are IntechOpen, the world's leading publisher of Open Access books Built by scientists, for scientists

6,900

Open access books available

185,000

International authors and editors

200M

Downloads

Our authors are among the

154

Countries delivered to

TOP 1%

most cited scientists

12.2%

Contributors from top 500 universities



WEB OF SCIENCE™

Selection of our books indexed in the Book Citation Index  
in Web of Science™ Core Collection (BKCI)

Interested in publishing with us?  
Contact [book.department@intechopen.com](mailto:book.department@intechopen.com)

Numbers displayed above are based on latest data collected.  
For more information visit [www.intechopen.com](http://www.intechopen.com)



# A Novel Electrochemical Sensor for the Detection of Reactive Red Dye to Determine Water Quality

*Rifat Kolatoğlu, Enes Aydın, Mehtap Demir, Ahmet Yıldız, Selcan Karakuş, Elif Tüzün, Nuray Beköz Üllen, Nevin Taşaltın and Ayben Kilislioglu*

## Abstract

In this study, tragacanth gum/chitosan/ZnO nanoprism-based electrochemical sensors were prepared for sensing reactive dyes in water. To use an electrochemical sensor, a ~250 nm-sized ZnO nanoprism was synthesized via ultrasonic-assisted green synthesis method, using tragacanth gum and chitosan polymer blend as a matrix. The electrochemical properties of tragacanth gum/chitosan/ZnO nanoprisms were compared against reactive red 35, reactive yellow 15, and reactive black 194. The electrochemical measurement results indicated that prepared tragacanth gum/chitosan/ZnO nanoprism-based electrochemical sensor detected 25 ppm reactive red 35 in 1 min at room temperature. This study reveals new high-potential novel tragacanth gum/chitosan/ZnO nanoprism-based sensing material for the detection of reactive red dye-consisted wastewater with high sensitivity and short response time.

**Keywords:** ZnO, chitosan, nanoprism, electrochemical sensor, environmental monitoring, reactive dye, wastewater

## 1. Introduction

The physicochemical properties of nanomaterials make them suitable candidates for sensor applications due to their high surface area and surfactant functional groups. Nanomaterials with different morphologies help to adapt their application-specific detection properties. Therefore, researchers focus on effective detection platforms (reaction time, sensitivity, and selectivity) for the detection of aqueous reactive dyes based on different detection principles with sensors prepared with different morphological structures of nanomaterials (nanoparticles, nanowires, nanoprisms, etc.). Also, the materials in nanoscale exhibit higher dissolution and higher solubility than in microscale. Many types of nanomaterials such as metal oxide semiconductors, carbon-based nanomaterials, graphene/graphene-based nanomaterials, and metal-organic frameworks have been investigated for sensing reactive dyes in water [1–15].

Electrochemical sensing method involves the measurement of the redox transformation of reactive dye molecules upon contact with the sensing nanomaterial

surface. The method mainly consists of (a) conductometric/resistive, (b) amperometric/voltammetric, and (c) impedimetric electrochemical sensing. Voltammetric sensors work based on the current difference between reference and working electrodes. This approach utilizes the measurement of current as a function of variation in the applied potential difference in terms of the oxidation or reduction of an electroresponses of an electrochemical sensor. The peak current measured during voltammetry-mediated oxidation of analyte (e.g., reactive dye) is reflected as a function of its concentration. The sensitivity of the voltammetric electrochemical sensor is defined as  $(I_g - I_0)/I_0$ , where  $I_g$  and  $I_0$  are the currents while sensing film - analyte (e.g., reactive dye) is interacting and not, respectively. The voltammetric-type electrochemical sensing allows the quantification of the redox state of analyte in terms of current variations [16–18].

Transducers of the electrochemical sensors have attractive attention for preparing highly sensitive sensors. Nonuniform ohmic drop on an electrochemical transducer significantly affects the cyclic voltammogram data. The shape of the cyclic voltammograms predicts various electrochemical transducer geometries and experimental conditions [19–35].

Zinc oxide (ZnO) nanomaterials have distinct properties such as high sensitivity, high surface area, nontoxic, good compatibility, specific shape, nanosize, and correspondingly high isoelectric point. The unique and adjustable properties of ZnO nanomaterials as n-type semiconductor materials show excellent chemical and thermal stability in a wide range of applications such as solar cells, optical devices, sensors, etc. As far as the morphological perspectives of ZnO are concerned, the synthesis and production procedures also play an important role. The different parameters such as surfactant, temperature, concentration, and time are very significant for the growth of nanomaterials with different morphologies in various synthesis processes. Numerous different methods have been reported worldwide for the synthesis of ZnO nanopowder, composites, and films with good surface structure. Noteworthy techniques for the synthesis of various ZnO nanomaterials are generally deposition, wet chemical technique, sol-gel treatment, hydrothermal process, solvothermal process, and microwave techniques [36, 37].

This is the first report of the preparation and structural characterization of novel tragacanth gum/chitosan/ZnO nanoprism and investigation of the voltammetric electrochemical sensing characteristics of tragacanth gum/chitosan/ZnO nanoprisms against reactive dyes in water towards environmental monitoring. We suggest that this tragacanth gum/chitosan/ZnO nanoprism material has a great potential for future applications in high-performance, low-cost, portable, small-scale voltammetric electrochemical sensors towards forthcoming electronics.

## 2. Materials and methods

### 2.1 Materials

Tragacanth gum (T) and chitosan were purchased from Sigma-Aldrich Company. Reactive red 35 (RR35), reactive yellow 15 (RY15), and acid black 194 (AB194) were obtained from Burboya Company. Zinc nitrate hexahydrate ( $\text{Zn}(\text{NO}_3)_2 \cdot 6\text{H}_2\text{O}$ ), glacial acetic acid (glacial 100%, pro analysis), and sodium hydroxide (NaOH) were purchased from Merck Company. MF-Millipore™ membrane filter was purchased from Merck Company. Ultrapure water was provided by a human ultrapure water system (water resistance: 18.3 Mohm) and was used for the preparation of all reactive dye solutions as analytes. All electrochemical gold transducers and voltammetric electrochemical workstation were purchased from Ebtro Electronics.

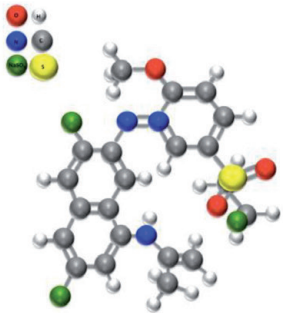
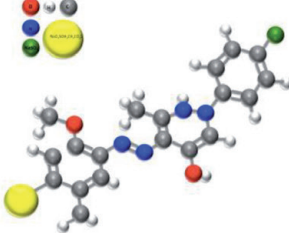
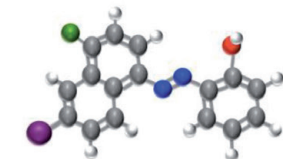
2.2 Synthesis of tragacanth gum/chitosan/ZnO nanoprism

Tragacanth gum/chitosan/ZnO nanoprisms were prepared using a green sonochemical method at 25°C (35 kHz frequency, 320 W, Sonoplus, Bandelin, Germany). In the first step, 0.1 g of tragacanth gum was dissolved in 50 ml of deionized pure water on a magnetic stirrer in 2 h at 25°C. In the second step, 0.1 g of chitosan was dissolved in 50 ml of 2% glacial acetic acid. In the third step, 25 ml of the prepared solutions was taken and mixed. In the fourth step, 0.1 M of Zn(NO<sub>3</sub>)<sub>2</sub>·6H<sub>2</sub>O and 0.2 M of NaOH was prepared in deionized pure water. In the fifth stage, the solution of Zn(NO<sub>3</sub>)<sub>2</sub>·6H<sub>2</sub>O was added in the solutions, and then the solution of NaOH was added dropwise under the sonicator at 25°C for 40 min (%30 amp). The solution was kept at 24 h in the dark at room temperature. Then, it was first filtered through membrane filters of 0.45 µm and 0.22 µm pore size, respectively. The final solution (viscosity: 1.28 cP and pH 4) was stored at 25°C for use in the sterile container for analysis.

2.3 Preparation and measurements of electrochemical sensors

Electrochemical gold transducers were rinsed with ultrapure water, dried with nitrogen gas, and coated with tragacanth gum/chitosan/ZnO nanoprism solution by dropping and drying the solution. The 3D model structure and the property of dyes used are shown in **Figure 1**.

The potential of the working electrode was varied linearly with time, while the reference electrode was maintained at a constant potential. The potential was

Dye	Molecular Formula	3D model structure	Molar mass (g mol <sup>-1</sup> )	λ <sub>max</sub> (nm)
Reactive Red 35	C <sub>12</sub> H <sub>18</sub> N <sub>3</sub> Na <sub>3</sub> O <sub>14</sub> S <sub>4</sub>		732.94	536
Reactive Yellow 15	C <sub>20</sub> H <sub>20</sub> N <sub>4</sub> Na <sub>2</sub> O <sub>11</sub> S		634.57	420
Reactive Black 194	C <sub>20</sub> H <sub>12</sub> N <sub>3</sub> NaO <sub>7</sub> S		461.38	233

**Figure 1.**  
*3D model structure and property of the reactive dyes.*

applied between the reference electrode and the working electrode, and the current was measured between the working electrode and the counter electrode. Ebtron voltammetric electrochemical workstation with a three-electrode configuration was used for all electrochemical tests. Cyclic voltammetry (CV) was performed in  $[-1, +1]$  V range with a scan rate of 50 mV/s.

### 3. Results and discussion

The structural analysis of the tragacanth gum/chitosan/ZnO nanoprism material was performed by X-ray diffraction (XRD) (**Figure 2**).

As seen in **Figure 2**, according to XRD analysis, strong peaks were observed at  $2\theta = 13^\circ, 31^\circ$ , which corresponds to the tragacanth gum/chitosan/ZnO crystalline planes. In the experiments, crystalline-structured tragacanth gum/chitosan/ZnO nanoprisms provided the advantage of obtaining a high surface area for higher interaction and reaction of sensing tragacanth gum/chitosan/ZnO nanoprism thin film on gold transducer-reactive dye with high electron mobility in terms of crystalline structure. SEM and EDX analyses of the prepared tragacanth gum/chitosan/ZnO nanoprisms were performed (**Figure 3**).

The EDX technique was employed to obtain some information on the spatial distribution of the corresponding elements. The EDX analysis of tragacanth gum/chitosan/ZnO nanoprisms provides the average percentage of zinc (Zn) and oxygen (O) at different points. All these suggest efficient preparation and presence of targeted atoms in tragacanth gum/chitosan/ZnO nanoprisms. The polymer matrix (tragacanth gum/chitosan) provides enormously large surface area for dispersion that helps ZnO to grow in the form of nanoprisms with higher reactivity for redox processing. The homogenous dispersion of ZnO in polymer matrix enhances conductivity and stability of the nanostructure. The complementary properties of tragacanth gum/chitosan/ZnO nanoprism generate a synergistic effect to enhance the electrochemical performance and provide improved charge exchange efficiency and stability during redox cycling.

Cyclic voltammetry measurements were performed to analyze the electrochemical sensor performance of tragacanth gum/chitosan/ZnO nanoprism-coated gold

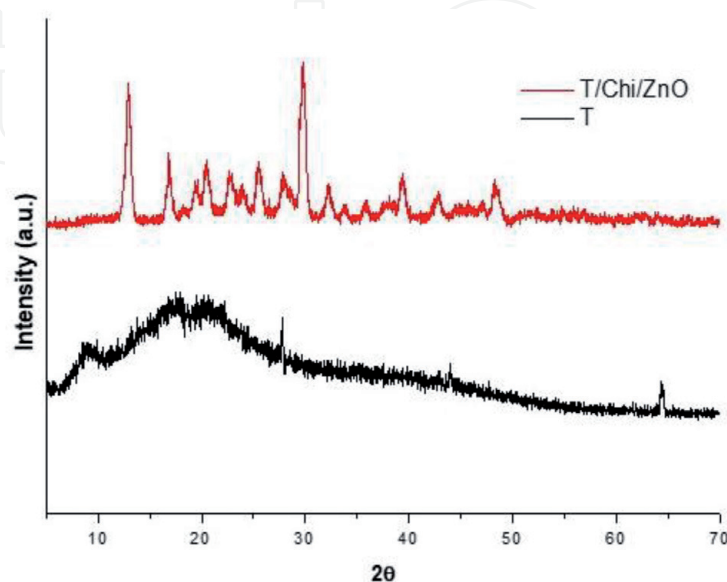


**Figure 2.**  
XRD analysis of tragacanth gum/chitosan/ZnO nanoprisms.



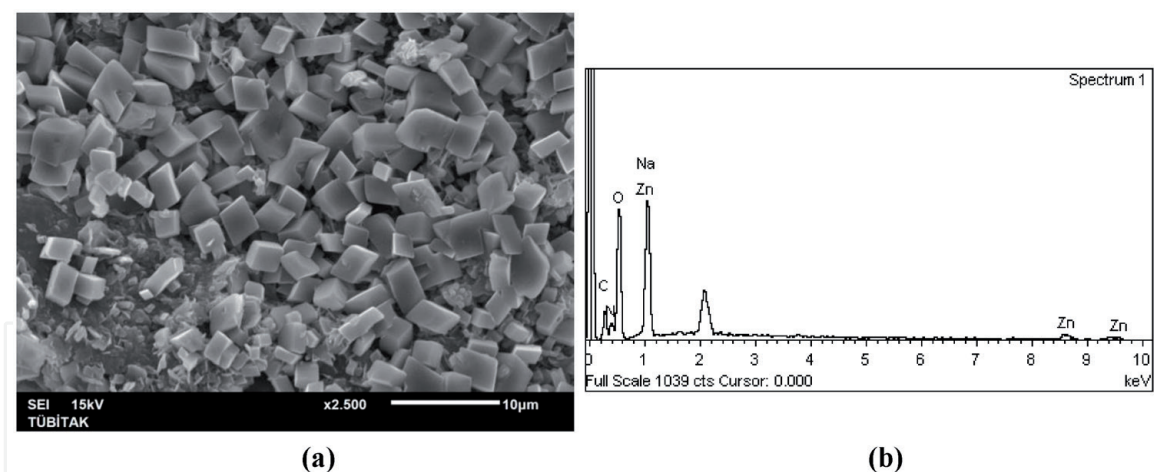
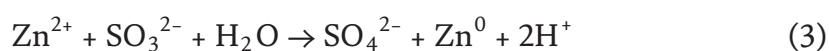
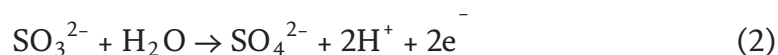
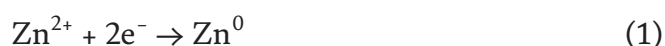


**Figure 3.**  
(a) SEM and (b) EDX analysis of tragacanth gum/chitosan/ZnO nanoprisms.

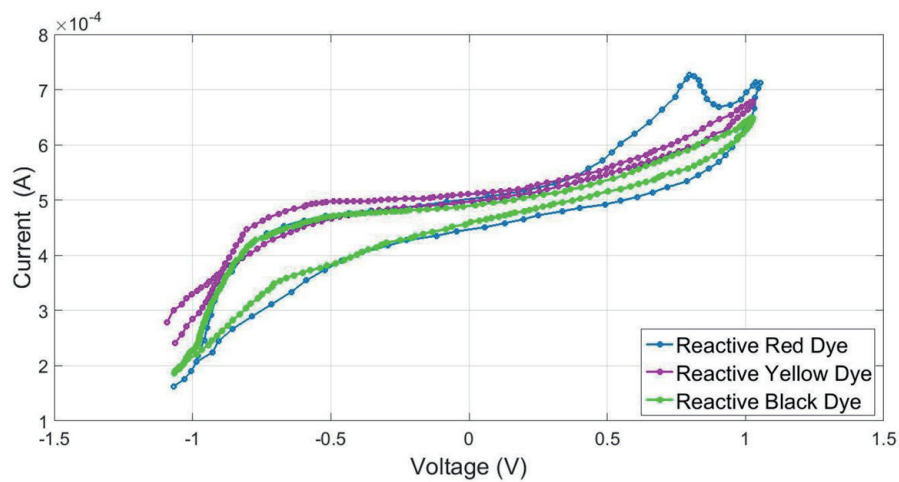
transducer. Current-voltage curves of tragacanth gum/chitosan/ZnO nanoprism-coated gold transducers against reactive red 35, reactive yellow 15, and reactive black 194 were obtained, respectively, in  $[-1, +10]$  V range with a scan rate of 50 mV/s at room temperature in real-time measurements by Ebtro voltammetric electrochemical workstation (**Figure 4**).

**Figure 4** shows the comparative current-voltage curves of tragacanth gum/chitosan/ZnO nanoprism-coated gold transducers against reactive red dye, reactive yellow dye, and reactive black dye in  $[-1, +10]$  V range with a scan rate of 50 mV/s at room temperature. The measured current responses were due to either oxidation or reduction of the reactive dye analytes over the entire cycle at the surface of the bare gold transducers. The current peaks arised from redox reactions between tragacanth gum/chitosan/ZnO nanoprism and reactive red dye molecules observed. The curves showed that there are no peaks arising from reactive yellow and black dye molecules as redox reactions did not occur between tragacanth gum/chitosan/ZnO nanoprism and reactive yellow and black dye molecules. The goal of this research was to evaluate the performance of the tragacanth gum/chitosan/ZnO nanoprism-coated gold transducer of the voltammetric electrochemical sensor in discriminating different reactive dyes in water. In this context, we focused on the electrochemical sensing capability tragacanth gum/chitosan/ZnO nanoprisms against to reactive dye-consisted water. The electrochemical oxidation of reactive red dye-consisted water was observed using the scan rate of 50 mV/s at room temperature over a potential range of  $-0.2$  to  $0.8$  V. In **Figure 4**, current-voltage curves of tragacanth gum/chitosan/ZnO nanoprism-coated gold transducer indicated a prominent redox peak for reactive red dye, while the other tragacanth gum/chitosan/ZnO nanoprism-coated gold transducers indicated no redox peak for reactive yellow and black dyes in water. The redox peak was attributed to a large number of  $\text{SO}_3^-$  branches of the reactive red 35 (Eqs. (1)–(3)).

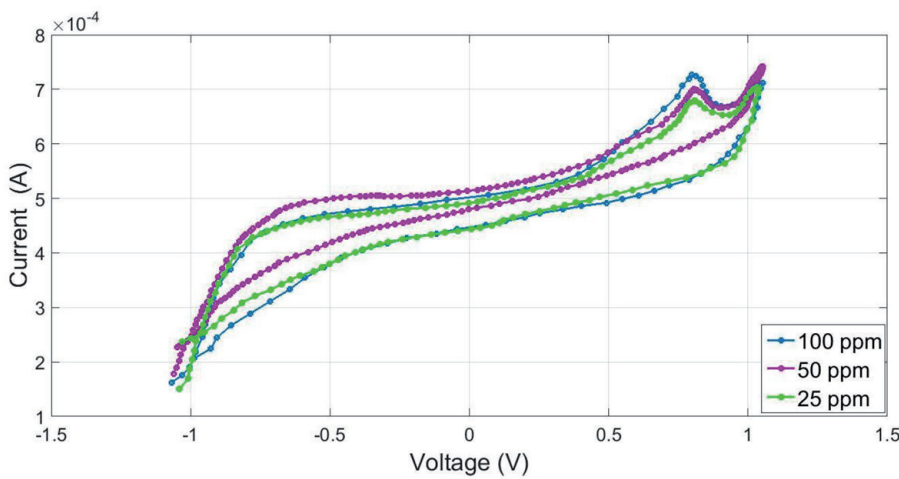


After these obtained results, sensor measurements were performed for determining reactive red dye. The different concentrations of reactive red dye were tested on tragacanth gum/chitosan/ZnO nanoprism-coated gold transducers in  $[-1, +10]$  V range with a scan rate of 50 mV/s at room temperature. Current peaks arised from redox reactions which came from between tragacanth gum/chitosan/ZnO nanoprism and reactive red dye molecules increased with increasing reactive red concentration in the range of 25–100 ppm. As the concentration of the reactive red dye molecules in the water increases, redox reactions increase the sensitivity of the sensor. Prepared tragacanth gum/chitosan/ZnO nanoprism-based electrochemical sensor detected 25 ppm reactive red dye in 1 min at room temperature.

The reproducibility of the tragacanth gum/chitosan/ZnO nanoprism-coated gold transducer was investigated by analyzing reactive red dye for four times. To ascertain the reproducibility results, the cyclic voltammetry experiments were carried out using the transducers under similar conditions. The peak currents for reactive red dye have not changed much even after a week. This showed the stability of the tragacanth gum/chitosan/ZnO nanoprism-coated gold transducer.



(a)



(b)

**Figure 4.** Current-voltage curves of tragacanth gum/chitosan/ZnO nanoprism-coated gold transducers against (a) reactive red dye, reactive yellow dye, and reactive black dye and (b) different reactive red dye concentrations in 25–100 ppm,  $[-1, +10]$  V range with a scan rate of 50 mV/s.

## 4. Conclusions

In this study, for environmental monitoring of reactive dye-consisting wastewater, the novel tragacanth gum/chitosan/ZnO nanoprism-based electrochemical sensor was prepared and tested via cyclic voltammetry technique. The electrochemical measurement results indicate that prepared tragacanth gum/chitosan/ZnO nanoprism-based electrochemical sensor has a higher sensitivity against reactive red dye than reactive yellow dye and reactive black dye in water. Prepared tragacanth gum/chitosan/ZnO nanoprism-based electrochemical sensor detected 25 ppm reactive red dye in 1 min at room temperature. This study reveals new high-potential sensing material for the detection of reactive dye-consisting wastewater with high sensitivity and short response time. It is the first time that the sensing interaction of tragacanth gum/chitosan/ZnO nanoprisms and reactive red dye was explained.

## Acknowledgements

This research was supported by TUBITAK Project 216M421.

## Author details

Rifat Kolatoğlu<sup>1</sup>, Enes Aydın<sup>1,2</sup>, Mehtap Demir<sup>1,3</sup>, Ahmet Yıldız<sup>4</sup>, Selcan Karakuş<sup>4</sup>, Elif Tüzün<sup>4</sup>, Nuray Beköz Üllen<sup>5</sup>, Nevin Taşaltın<sup>1,6\*</sup> and Ayben Kilislioğlu<sup>4</sup>

1 Department of Electrical-Electronics Engineering, Sensor Technology Laboratory, Maltepe University, Istanbul, Turkey

2 ABB Electronics, Istanbul, Turkey

3 Department of Metallurgy and Material Engineering, Adiyaman University, Adiyaman, Turkey

4 Department of Chemistry, İstanbul University-Cerrahpaşa, Istanbul, Turkey

5 Department of Metallurgical and Materials Engineering, İstanbul University-Cerrahpaşa, Istanbul, Turkey

6 Department of Renewable Energy Technology, Maltepe University, Istanbul, Turkey

\*Address all correspondence to: [nevintasaltin@maltepe.edu.tr](mailto:nevintasaltin@maltepe.edu.tr)

## IntechOpen

© 2020 The Author(s). Licensee IntechOpen. This chapter is distributed under the terms of the Creative Commons Attribution License (<http://creativecommons.org/licenses/by/3.0>), which permits unrestricted use, distribution, and reproduction in any medium, provided the original work is properly cited. 



## References

- [1] Hou SC, Zhang AY, Su M. Nanomaterials for biosensing applications. *Nanomaterials*. 2016;**6**:58
- [2] Rowland CE, Brown CW, Delehanty JB, Medintz IL. Nanomaterial-based sensors for the detection of biological threat agents. *Materials Today*. 2016;**19**:464-477
- [3] Saravanakumar B, Kim SJ. Growth of 2D ZnO nanowall for energy harvesting application. *Journal of Physical Chemistry C*. 2014;**118**:8831-8836
- [4] He JH, Hsin CL, Liu J, Chen LJ, Wang ZL. Piezoelectric gated diode of a single ZnO nanowire. *Advanced Materials*. 2007;**19**:781-784
- [5] Purusothaman Y, Alluri NR, Chandrasekhar A, Kim SJ. Elucidation of the unsymmetrical effect on the piezoelectric and semiconducting properties of Cd-doped 1D-ZnO nanorods. *Journal of Materials Chemistry C*. 2017;**5**:415-426
- [6] Ramadoss A, Kim SJ. Facile preparation and electrochemical characterization of graphene/ZnO nanocomposite for supercapacitor applications. *Materials Chemistry and Physics*. 2013;**140**:405-411
- [7] Brozek CK, Zhou D, Liu H, Li X, Kittilstved KR, Gamelin DR. A review on ZnO nanostructured materials: Energy, environmental and biological applications. *Nano Letters*. 2018;**18**:3297-3302
- [8] Pullagurala VLR, Adisa IO, Rawat S, Kim B, Barrios AC, Velo IAM, et al. Finding the conditions for the beneficial use of ZnO nanoparticles towards plants—A review. *Environmental Pollution*. 2018;**241**:1175-1181
- [9] Theerthagiri J, Chandrasekaran S, Sunitha S, Elakkiya V, Nithyadharseni P, Senthil RA, et al. Recent developments of metal oxide based heterostructures for photocatalytic applications towards environmental remediation. *Journal of Solid State Chemistry*. 2018;**267**:35-52
- [10] Theerthagiri J, Karuppasamy K, Durai G, Rana AHS, Arunachalam P, Sangeetha K, et al. Recent advances in metal chalcogenides (MX; X = S, Se) nanostructures for electrochemical supercapacitor applications: A brief review. *Nanomaterials*. 2018;**8**:256
- [11] Qi K, Cheng B, Yu J, Ho W. Review on the improvement of the photocatalytic and antibacterial activities of ZnO. *Journal of Alloys and Compounds*. 2017;**727**:792-820
- [12] SoYoon S, Ramadoss A, Saravanakumar B, Kim SJ. Novel Cu/CuO/ZnO hybrid hierarchical nanostructures for non-enzymatic glucose sensor application. *Journal of Electroanalytical Chemistry*. 2014;**717**:90-95
- [13] Alam U, Khan A, Raza W, Khan A, Bahnemann D, Muneer M. Highly efficient Y and V co-doped ZnO photocatalyst with enhanced dye sensitized visible light photocatalytic activity. *Catalysis Today*. 2017;**284**:169-178
- [14] Mohan R, Krishnamoorthy K, Kim SJ. Enhanced photocatalytic activity of Cu-doped ZnO nanorods. *Solid State Communications*. 2012;**152**:375-380
- [15] Theerthagiri J, Senthil RA, Senthilkumar B, Polu AR, Madhavan J, Ashokkumar M. Recent advances in MoS<sub>2</sub> nanostructured materials for energy and environmental applications—A review. *Journal of Solid State Chemistry*. 2017;**252**:43-71
- [16] Wang XS, Zhang JB, He Y, Wang LY, Liu L, Wang H, et al. Porous

Nd-doped In<sub>2</sub>O<sub>3</sub> nanotubes with excellent formaldehyde sensing properties. *Chemical Physics Letters*. 2016;**658**:319-323

[17] Stradiotto NR, Yamanaka H, Zanon MVB. Electrochemical sensors: A powerful tool in analytical chemistry. *Journal of the Brazilian Chemical Society*. 2003;**14**:159-173

[18] Wang Q, Zheng JB, Zhang HF. A novel formaldehyde sensor containing AgPd alloy nanoparticles electrodeposited on an ionic liquid-chitosan composite film. *Journal of Electroanalytical Chemistry*. 2012;**674**:1-6

[19] Švancara I, Vytrás K, Kalcher K, Walcarius A, Wang J. Carbon paste electrodes in facts, numbers, and notes: A review on the occasion of the 50-years jubilee of carbon paste in electrochemistry and electroanalysis. *Electroanalysis*. 2009;**21**:7-28

[20] Zima J, Švancara I, Barek J, Vytrás K. Recent advances in electroanalysis of organic compounds at carbon paste electrodes. *Critical Reviews in Analytical Chemistry*. 2009;**39**:204-227

[21] Vyskocil V, Barek J. Mercury electrodes—Possibilities and limitations in environmental electroanalysis. *Critical Reviews in Analytical Chemistry*. 2009;**39**:189-203

[22] Stetter JR, Li J. Amperometric gas sensors—A review. *Chemical Reviews*. 2008;**108**:352-366

[23] Yogeswaran U, Chen SM. A review on the electrochemical sensors and biosensors composed of nanowires as sensing material. *Sensors*. 2008;**8**:290-313

[24] Mays DE, Hussam A. Voltammetric methods for determination and speciation of inorganic arsenic in the

environment—A review. *Analytica Chimica Acta*. 2009;**646**:6-16

[25] Bobrowski A, Królicka A, Zarębski J. Characteristics of voltammetric determination and speciation of chromium—A review. *Electroanalysis*. 2009;**12**:1449-1458

[26] Amatore C, Oleinick A, Svir I. Theoretical analysis of microscopic ohmic drop effects on steady-state and transient voltammetry at the disk microelectrode: A quasi-conformal mapping modeling and simulation. *Analytical Chemistry*. 2008;**80**:7947-7956

[27] Amatore C, Oleinick AI, Svir I. Numerical simulation of diffusion processes at recessed disk microelectrode arrays using the quasi-conformal mapping approach. *Analytical Chemistry*. 2009;**81**:4397-4405

[28] Guo JD, Lindner E. Cyclic voltammograms at coplanar and shallow recessed microdisk electrode arrays: Guidelines for design and experiment. *Analytical Chemistry*. 2009;**81**:130-138

[29] Douglass EF, Driscoll PF, Liu DL, Burnham NA, Lambert CR, McGimpsey WG. Effect of electrode roughness on the capacitive behavior of self-assembled monolayers. *Analytical Chemistry*. 2008;**80**:7670-7677

[30] Menshykau D, Compton RG. The influence of electrode porosity on diffusional cyclic voltammetry. *Electroanalysis*. 2008;**20**:2387-2394

[31] Bae JH, Lim YR, Jung W, Silbey RJ, Sung J. Practical model for imperfect conductometric molecular wire sensors. *Analytical Chemistry*. 2009;**81**:578-583

[32] Lee CY, Bond AM. Evaluation of levels of defect sites present in highly ordered pyrolytic graphite electrodes using capacitive and faradaic current components derived

simultaneously from large-amplitude Fourier transformed ac voltammetric experiments. *Analytical Chemistry*. 2009;**81**:584-594

[33] Sheth DB, Diefes R, Gratzl M. Spatially averaging electrodes. *Analytical Chemistry*. 2009;**81**:2129-2134

[34] Ogurtsov VI, Beni V, Strutwolf J, Arrigan DWM. Study of the effects of nonlinear potential sweeps on voltammetry. *Electroanalysis*. 2009;**21**:68-76

[35] Rajendra NG, Vinod KG, Neeta B, Ram AS. Electrochemical sensor for the determination of dopamine in presence of high concentration of ascorbic acid using a Fullerene-C60 coated gold electrode. *Electroanalysis*. 2008;**20**(7):757-764

[36] Meulenkamp EA. Synthesis and growth of ZnO nanoparticles. *The Journal of Physical Chemistry. B*. 1998;**102**:5566-5572

[37] Radzimska AK, Jesionowski T. Zinc oxide-from synthesis to application: A review. *Materials*. 2014;**7**:2833-2881